SUPPLEMENTAL DATA

Lee and Foskett, "Requirement for cAMP-activated Ca^{2+} signaling for CFTR-mediated porcine and human airway submucosal gland serous cell fluid secretion."

FIGURE LEGENDS

Supplemental Figure 1. VIP and forskolin stimulated cell shrinkage is linearly correlated with changes in SPQ fluorescence in adult porcine bronchial serous acinar cells. (**A-B**) Representative traces showing changes in SPQ fluorescence (normalized to fluorescence at time = 0 [$F/F_{t=0}$]; black inverted triangles) and normalized cell volume (red circles) in response to 1 μM VIP (*A*) and 10 μM forskolin (*B*).

Supplemental Figure 2. Solute uptake during VIP stimulation is mediated by NKCC and paired NHE/AE activity in porcine bronchial serous acinar cells. (**A**) Stimulation of control serous cells (no inhibitors) with 1 μM VIP in 0-Ca^{2+}_o solution caused transient $[Ca^{2+}]_i$ and shrinkage responses. Peak $[Ca^{2+}]_i$ elevation was 98 ± 5 nM (n = 7). $[Ca^{2+}]_i$ returned to baseline levels after 140 ± 17 sec (as discussed in text). The time 50% volume recovery was 187 ± 28 sec (n = 7) after peak shrinkage. (**B**) VIP/0-Ca^{2+}_o stimulation in the presence of 100 μM bumetanide (an NKCC inhibitor) significantly inhibited the rate of cell swelling (time to 50% volume recovery = 404 ± 69 sec; n = 4; $p < 0.05$ compared with control by Dunnett's test). Peak $[Ca^{2+}]_i$ elevation was 99 ± 6 nM and $[Ca^{2+}]_i$ returned to resting levels after 149 ± 18 sec, while cells shrank by 19 ± 1 % within 103 ± 16 sec after the onset of the $[Ca^{2+}]_i$ response (all $[Ca^{2+}]_i$ and shrinkage values n.s. compared with control by Student's t test or Dunnett's test). (**C**) Stimulation of serous cells with VIP/0-Ca^{2+}_o in the presence of 30 μM DMA (an NHE inhibitor) inhibited the rate of cell swelling similar to that observed in presence of bumetanide (time to 50% volume recovery = 384 ± 86 sec; n = 4; $p < 0.05$ compared with control by Dunnett's test; n.s. compared with bumetanide). Peak $[Ca^{2+}]_i$ elevation was 103 ± 11 nM and $[Ca^{2+}]_i$ returned to resting levels after 165 ± 31 sec, while cells shrank by 18 ± 1 % within 113 ± 18 sec after the onset of the $[Ca^{2+}]_i$ response (all $[Ca^{2+}]_i$ and shrinkage values n.s. compared with control by Dunnett's test). (**D**) Serous cells stimulated with VIP/0-Ca^{2+}_o in presence of both 30 μM DMA and 100 μM bumetanide had inhibited rate of cell swelling exceeding that observed in presence of either drug alone (time to 50 % volume recovery = 731 ± 111 sec; n = 4; $p < 0.01$ compared with control by Dunnett's test; $p < 0.05$ compared with either DMA or bumetanide). Peak $[Ca^{2+}]_i$

elevation was 92 ± 11 nM and $[Ca^{2+}]_i$ returned to resting levels after 166 ± 39 sec, while cells shrank by 19 ± 1 % within 93 ± 16 sec after the onset of the $[Ca^{2+}]_i$ response (all $[Ca^{2+}]_i$ and shrinkage values n.s. compared with control by either Student's t test or Dunnett's test). (**E**) Summaries of time to 50% volume recovery under control conditions or in the presence of bumetanide and/or DMA. Results indicate that NKCC and paired NHE/AE activity contribute to Cl^- uptake during VIP-induced Cl^- secretion, as observed during CCh stimulation (4). Asterisks indicate significance compared with control cells (Dunnett's test; * = $p < 0.05$; ** = $p < 0.01$). (**F**) After stimulation with VIP in 0-Ca^{2+}_o, volume recovery was completely blocked when extracellular Na^+ was isosmotically replaced with impermeant *N*-methyl-*D*-glucamine ($NMDG^+$).

Supplemental Figure 3. **VIP/forskolin-induced porcine bronchial serous cell shrinkage is inhibited by GlyH-101 and $CFTR_{inh}172$, but not by NFA.** (**A**) As discussed in text, control cells shrank by 15 ± 2 % within 49 ± 11 sec (n = 6) during stimulation with 10 μM forskolin (representative trace shown in top panel). GlyH-101 (10 μM) inhibited forskolin-induced cell shrinkage response to 10 ± 2 % (n.s. compared with control by Dunnett's test) within 210 ± 53 sec (n = 7; $p < 0.05$ compared with control by Dunnett's test) (bottom panel). Values summarized in *C*. (**B**) Control cells stimulated with 1 μM VIP shrank by 15 ± 2 % within 107 ± 30 sec (representative trace shown in top panel). GlyH-101 (10 μM) inhibited VIP-induced cell shrinkage response to 11 ± 2 % (n.s. compared with control by Dunnett's test) within 361 ± 141 sec ($p < 0.05$ compared with control by Dunnett's test; n = 4). (**C**) Summaries of peak cell shrinkage (left) and time to peak shrinkage (right) during forskolin or VIP stimulation in control and GlyH-101- and NFA-treated cells (* = $p < 0.05$). In contrast to GlyH-101, 50 μM NFA had no effect on shrinkage magnitude or kinetics upon stimulation with forskolin (14 ± 1 % within 65 ± 7 sec; n = 7; both values n.s. compared with control by Dunnett's test) or VIP (16 ± 2 within 99 ± 45 sec; n = 4, both values n.s. compared with control by Dunnett's test). (**D**) The CFTR inhibitor $CFTR_{inh}172$ (10 μM) completely abolished forskolin- and VIP-induced shrinkage (*D and E*, respectively), but did not block CCh-stimulated cell shrinkage. The peak $[Ca^{2+}]_i$ responses in the presence of GlyH-101 (123 ± 16 nM and 137 ± 30 nM in response to forskolin and VIP, respectively), NFA (139 ± 15 nM and 145 ± 10 nM in response to forskolin and VIP, respectively), or $CFTR_{inh}172$ (125 ± 23 and 119 ± 14 in response to forskolin and VIP, respectively) were not significantly different from those observed in the absence of GlyH-101/NFA (reported in text), suggesting inhibition of cell shrinkage by GlyH-101 and $CFTR_{inh}172$ is not due to inhibition of Ca^{2+} signals but rather by inhibition of CFTR-mediated Cl^- efflux, in agreement with data from Wt and $CFTR^{-/-}$ tracheal gland serous cells (Fig. 2). The stronger

shrinkage inhibition by 10 μM $CFTR_{inh}172$ compared with 10 μM GlyH-101 agrees with NO_3^- substitution experiments suggesting $CFTR_{inh}172$ is a stronger inhibitor of VIP-stimulated anion permeability at these concentrations (Fig. 3).

Supplemental Figure 4. CCh-stimulated secretion is intact in *CFTR*$^{-/-}$ porcine tracheal gland serous cells. (**A**) Representative traces of $[Ca^{2+}]_i$ and cell volume responses of WT (left) and *CFTR*$^{-/-}$ (right) serous acinar cells stimulated with 250 nM CCh. Peak $[Ca^{2+}]_i$ were 197 ± 12 nM within 46 ± 8 sec (WT; n = 12) and 205 ± 14 nM within 37 ± 5 sec (*CFTR*$^{-/-}$; n = 5; n.s. compared with WT), followed by plateau $[Ca^{2+}]_i$ of 127 ± 10 (Wt; n = 12) and 150 ± 12 nM (*CFTR*$^{-/-}$; n = 5; n.s.). Cell shrinkage was 8 ± 1 % within 69 ± 10 sec (Wt; n = 11) and 9 ± 1 % within 64 ± 16 sec (*CFTR*$^{-/-}$; n = 5; all values n.s.). (**B**) Representative traces of $[Ca^{2+}]_i$ and cell volume responses of WT (left) and *CFTR*$^{-/-}$ (right) serous acinar cells stimulated with 500 μM CCh. Peak $[Ca^{2+}]_i$ responses were 283 ± 29 nM within 60 ± 8 sec (Wt; n = 15) and 264 ± 14 nM within 64 ± 18 sec (*CFTR*$^{-/-}$; n = 5; n.s.), followed by plateau $[Ca^{2+}]_i$ of 207 ± 17 nM (WT; n = 15) and 225 ± 9 nM (*CFTR*$^{-/-}$; n = 4; n.s.). Cell shrinkage was 19 ± 1 % within 48 ± 6 sec (Wt; n = 14) and 22 ± 2 % within 41 ± 7 sec (*CFTR*$^{-/-}$; n = 5; all values n.s.). (**C**) Representative traces of $[Ca^{2+}]_i$ and cell volume responses of WT (left) and *CFTR*$^{-/-}$ (right) serous acinar cells stimulated with 1 μM CCh, peak $[Ca^{2+}]_i$ responses were 351 ± 10 nM within 50 ± 7 sec (Wt; n = 10) and 359 ± 16 nM within 42 ± 4 sec (*CFTR*$^{-/-}$; n = 7; n.s.), followed by a plateau $[Ca^{2+}]_i$ elevation to 267 ± 17 nM (WT; n = 10) and 277 ± 9 (*CFTR*$^{-/-}$; n = 7; n.s.) Cell shrinkage was 20 ± 1 % within 41 ± 6 sec (Wt; n = 10) and 21 ± 2 % within 33 ± 6 sec (*CFTR*$^{-/-}$; n = 6; all values n.s.). (**D-F**) Summaries of CCh-evoked cell shrinkage (*E* and *E*) and $[Ca^{2+}]_i$ responses (*F*).

Supplemental Figure 5. Raw traces of NO_3^- substitution experiments performed in porcine bronchial serous acinar cells. (**A–H**) SPQ- and BAPTA-loaded cells were imaged in 0-HCO_3^- solution as described in text. SPQ fluorescence was monitored during substitution of extracellular Cl^- with NO_3^- in 0-Ca^{2+}_o with 100 μM bumetanide. The derivative of the fluorescence trace was measured immediately after NO_3^- substitution in each experiment, to calculate the initial rate of SPQ fluorescence change ($F/F_{t=0} \cdot sec^{-1}$). In absence of VIP (*A*), SPQ fluorescence changed by 0.003 ± 0.001 $F/F_{t=0}$ units • sec^{-1} (n = 7). After stimulation with 1 μM VIP (*B*), fluorescence changed by 0.035 ± 0.005 $F/F_{t=0}$ units • sec^{-1} (*B*; >10-fold increase compared with no VIP; $p < 0.01$; n = 7). After 1 μM VIP in the presence of 100 μM NFA (*C*), fluorescence changed by 0.028 ± 0.003 $F/F_{t=0}$ units • sec^{-1} (n.s. compared with VIP alone, $p < 0.01$ compared with no VIP; n = 4). After 1 μM VIP in the presence of 10 μM GlyH-101 (*D*),

fluorescence changed by 0.013 ± 0.001 $F/F_{t=0}$ units • sec^{-1} ($p < 0.01$ compared with VIP only or no VIP; n = 5). After 1 μM VIP in the presence of 30 μM GlyH-101 (*E*), fluorescence changed by 0.006 ± 0.001 ($p < 0.01$ compared with VIP only; $p < 0.05$ compared with 10 μM GlyH-101; n.s. compared with no VIP; n = 5). After 1 μM VIP in the presence of 10 μM $CFTR_{inh}172$ (*F*), fluorescence changed by 0.004 ± 0.001 $F/F_{t=0}$ units • sec^{-1} (n.s. compared with no VIP, $p < 0.01$ compared with VIP only; n = 9). After stimulation with 100 nM VIP (*G*), fluorescence changed by 0.025 ± 0.003 $F/F_{t=0}$ units • sec^{-1} (n = 8; n.s. compared with 1 μM VIP). After stimulation with 10 μM forskolin (*H*), fluorescence changed by 0.031 ± 0.005 $F/F_{t=0}$ units • sec^{-1} (n = 5; n.s. compared with 1 μM VIP). (**I**) Summary of average rates from experiments as shown in *A*-*H*. (**J**) Representative traces of SPQ fluorescence during NO_3^- substitution in absence (left) and presence (right) of 100 nM CCh. Experiments carried out in 0-HCO_3^- with 100 μM bumetanide as above, except for the presence of 1.2 mM $Ca^{2+}{}_o$ and absence of BAPTA. Peak $[Ca^{2+}]_i$ elevation (~ 110 nM in 25-30 % of cells) during 100 nM CCh stimulation would be expected to occur ~ 80-100 sec after stimulation (4). If this were sufficient to activate a Cl^- permeability, it would be expected to be correlated with an increased rate of SPQ fluorescence change in 30-40% of cells. No increase in fluorescence change was observed in 40 cells/acini stimulated with 100 nM CCh, suggesting 100 nM CCh alone is not sufficient to activate Cl^- permeability. (**K**) Average of traces of experiments as in *J*, showing mean SPQ fluorescence changes during NO_3^- substitution in the absence (left; n = 8) and presence (right; n = 40) of 100 nM CCh.

Supplemental Figure 6. Resting $[Cl^-]_i$ is identical in WT and *CFTR*$^{-/-}$ neonatal porcine tracheal gland serous acinar cells. (**A-B**) Representative traces of SPQ calibrations performed in Wt (*A*) and *CFTR*$^{-/-}$ (*B*) cells. At beginning of each experiment, cells were exposed to normal extracellular HCO_3^- buffer to determine resting SPQ fluorescence. Solution was then exchanged for a HEPES-buffered solution containing 10 μM nigericin and 10 μM tributyltin to clamp $pH_i = pH_o$ and $[Cl^-]_i = [Cl^-]_o$ along with various known $[Cl^-]$ (0, 30, 70, or 140 mM) to determine the relationship between SPQ fluorescence and $[Cl^-]_i$. Solutions identical to those described in (3, 4). (*C*-*D*) Using data from experiments performed as in *A*-*B* (n = 5 for each genotype), composite Stern-Volmer plots were constructed. Fluorescence at 0-Cl^- ($F_{0\text{-}Cl\text{-}}$) was normalized to 1 and divided by fluorescence at the various $[Cl^-]$ ($F_{0\text{-}Cl\text{-}}/F$). Linear regression fits (red solid lines) to the raw data (red circles) revealed a Stern-Volmer quenching constant (K_{SV}) of 18 M^{-1} in WT cells and 17 M^{-1} in *CFTR*$^{-/-}$ cells. The equation of the line fit to the WT data was $y = (0.018 \pm 0.001)x + (1.02 \pm 0.09)$. The equation of the line fit to the *CFTR*$^{-/-}$ data was $y = (0.0017 \pm 0.001)x + (1.00 \pm 0.07)$. The $F_{0\text{-}Cl\text{-}}$ values were not used, as their normalization to 1

would artificially constrain fit. SPQ fluorescence values at beginning of each experiment (F_{rest}) indicate that resting $[Cl^-]_i$ was 63 ± 6 mM in Wt cells ($F_{0\text{-}Cl\text{-}}/F_{rest}$ = 2.15 ± 0.1) and 66 ± 5 mM in *CFTR*$^{-/-}$ cells ($F_{0\text{-}Cl\text{-}}/F_{rest}$ = 2.13 ± 0.1; both values n.s.). Similar resting $[Cl^-]_i$ in Wt and *CFTR*$^{-/-}$ cells agrees with data in Figure 3*C-F* sugesting these cells have similar resting Cl^- permeability.

SUPPLEMENTAL FIGURE 1

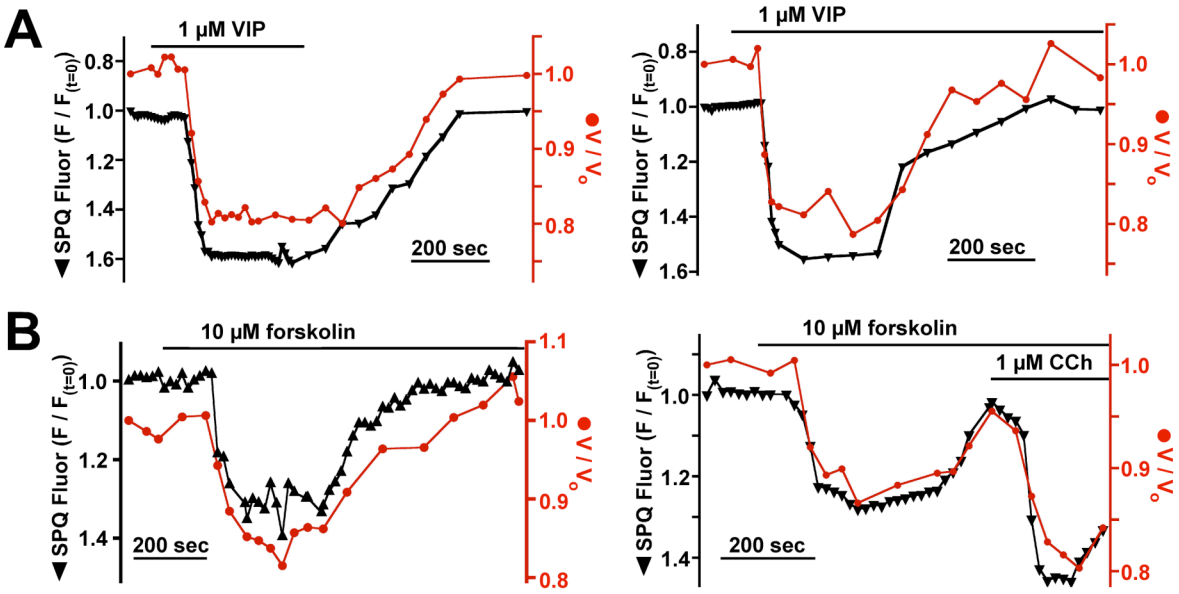

SUPPLEMENTAL FIGURE 2

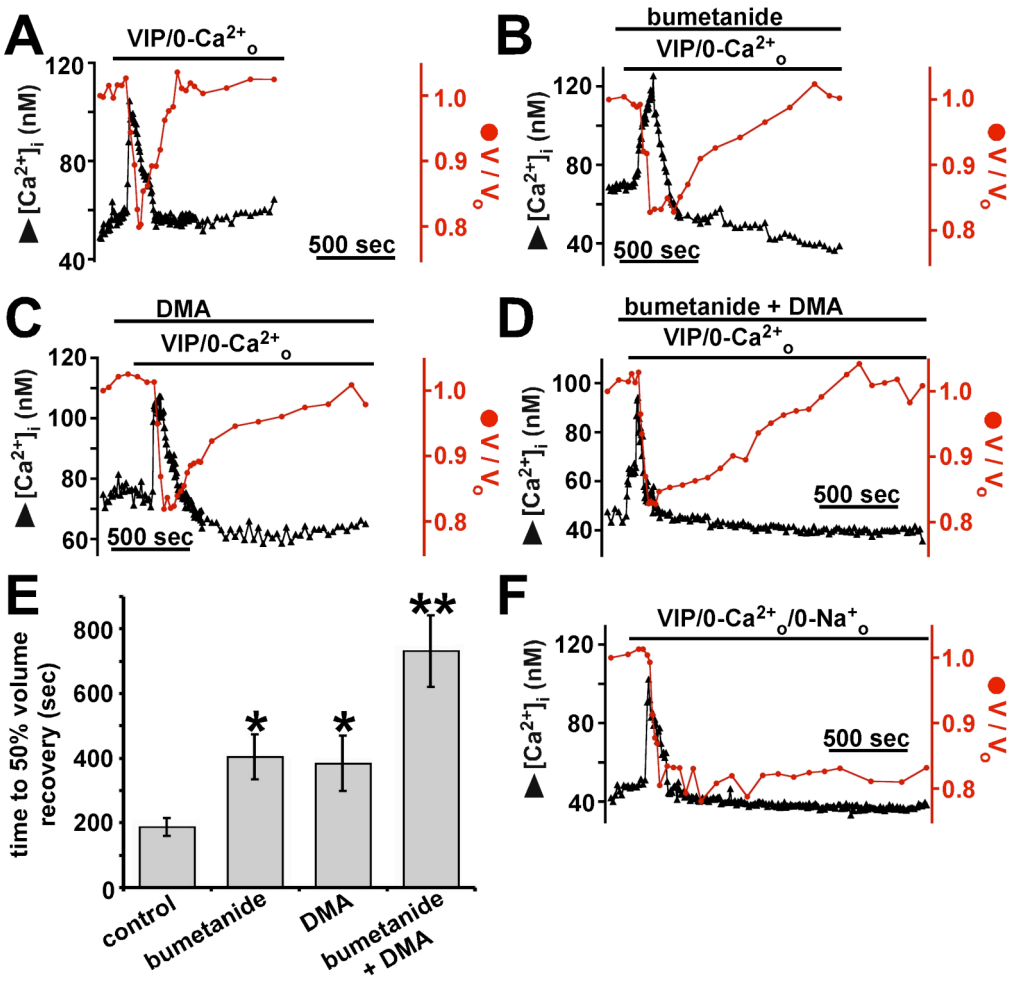

SUPPLEMENTAL FIGURE 3

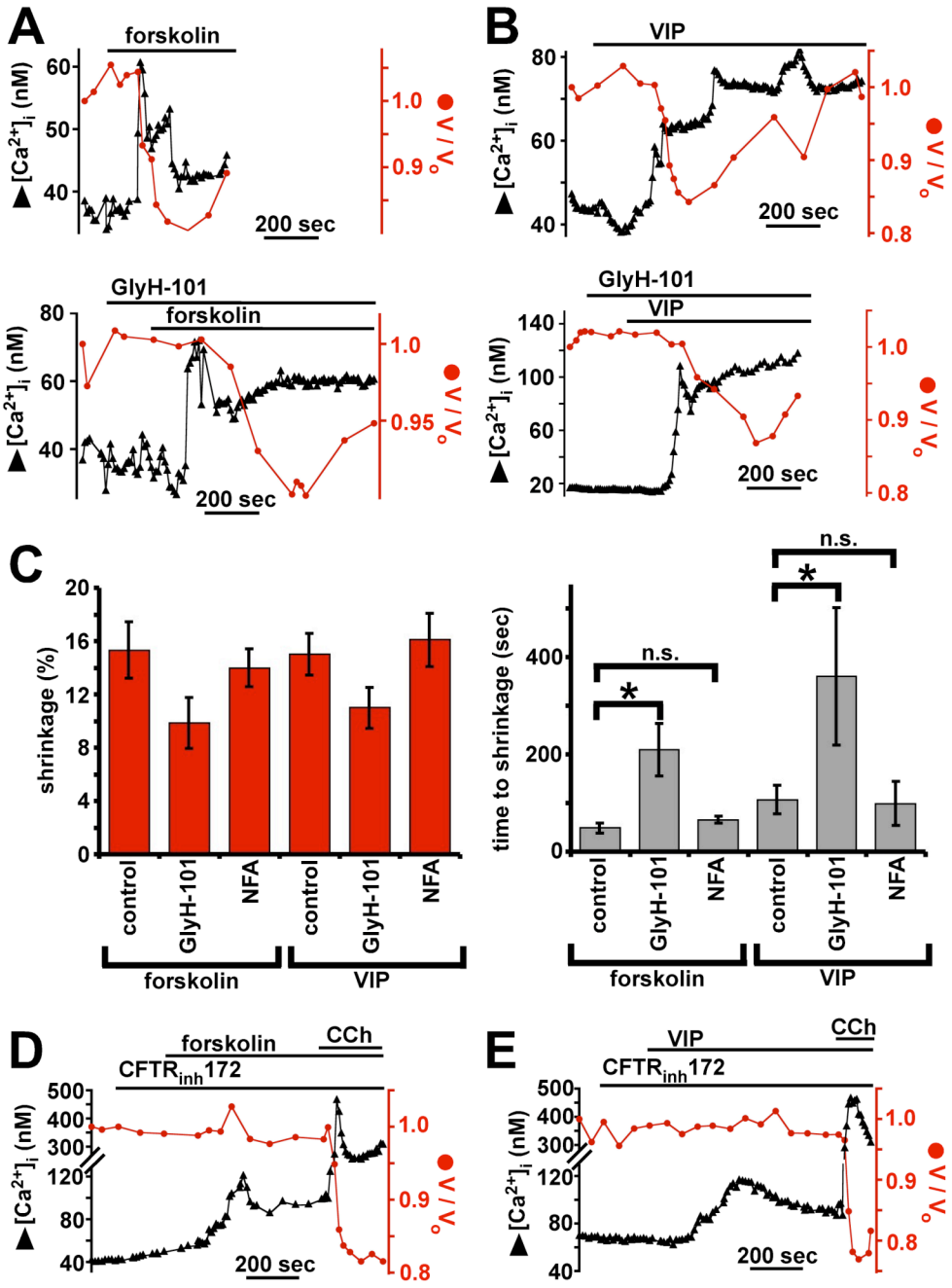

SUPPLEMENTAL FIGURE 4

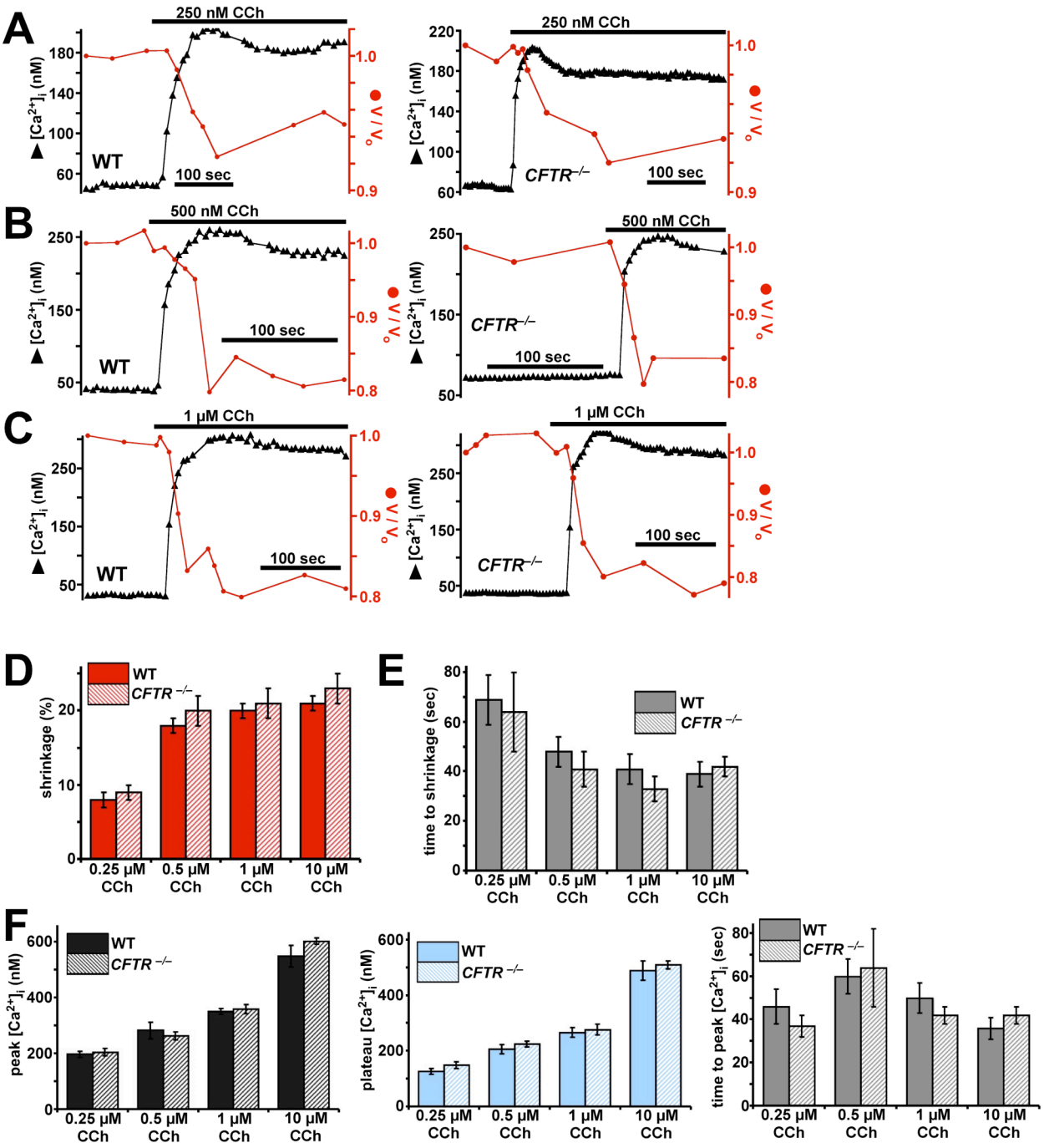

SUPPLEMENTAL FIGURE 5

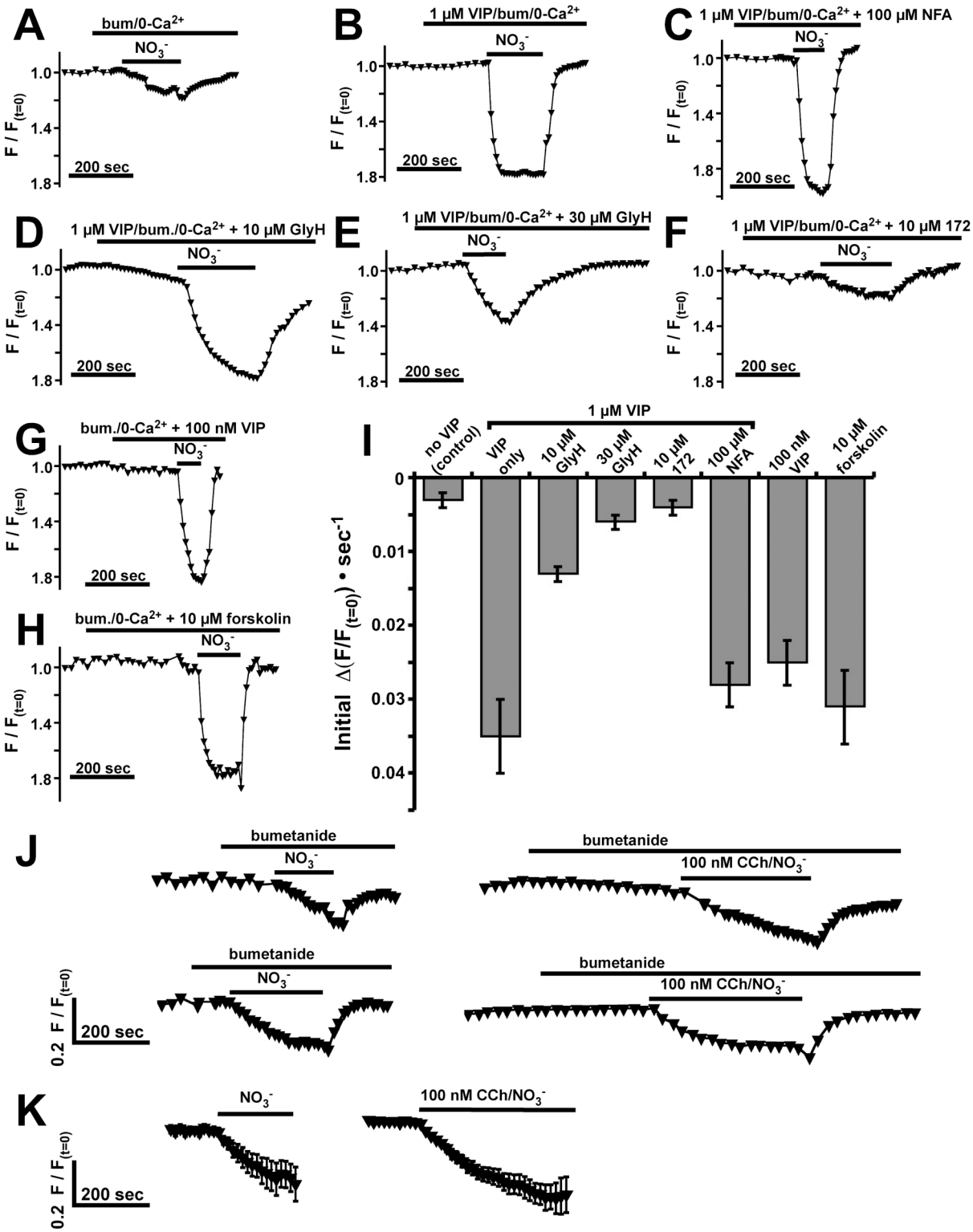

SUPPLEMENTAL FIGURE 6